miR-141 impairs mitochondrial function in cardiomyocytes subjected to hypoxia/reoxygenation by targeting Sirt1 and MFN2

HAO ZHANG[1], YAQIAO WANG[1], KEHAN WU[1], RUNMIN LIU[1], HAO WANG[1], YONGWEI YAO[1], PETER KVIETYS[2] and TAO RUI[1,3-5]

[1]Division of Cardiology, Department of Medicine, The Affiliated People's Hospital of Jiangsu University, Zhenjiang, Jiangsu 212002, P.R. China; [2]Department of Physiological Sciences, College of Medicine, Alfaisal University, Riyadh 11533, Saudi Arabia; [3]Critical Care Western, Schulich School of Medicine and Dentistry, Western University, London, ON N6A 5C1; [4]Critical Illness Research, Lawson Health Research Institute, London, ON N6A 4G5; [5]Departments of Medicine, Pathology and Laboratory Medicine, Schulich School of Medicine and Dentistry, Western University, London, ON N6A 5C1, Canada

Received May 27, 2022; Accepted October 4, 2022

DOI: 10.3892/etm.2022.11699

Abstract. Mitochondrial oxidative stress and dysfunction are major pathogenic features of cardiac injury induced by ischemia/reperfusion (I/R). MicroRNA-141 (miR-141) has been implicated in the mitochondrial dysfunction in cell-based models of oxidant stress. Thus, the main aim of the present study was to systematically assess the role of miR-141 in cardiomyocyte injury induced by simulated I/R. The challenge of HL-1 cardiomyocytes with hypoxia/reoxygenation (H/R) decreased cell viability, which was also associated with an increase in miR-141 expression. The H/R-induced cell injury was mitigated by a miR-141 inhibitor and exacerbated by a miR-141 mimic. Furthermore, H/R induced mitochondrial superoxide production, dysfunction (decreased oxygen utilization and membrane depolarization), as well as ultrastructural damage. These mitochondrial effects were mitigated by a miR-141 inhibitor and intensified by a miR-141 mimic. Luciferase reporter assay, reverse transcription-quantitative PCR, and western blot analyses identified sirtuin-1 (Sirt1) and mitofusin-2 (MFN2) as targets of miR-141. The silencing of Sirt1 reduced the MFN2 cardiomyocyte levels and reversed the alleviating effects of miR-141 inhibitor on mitochondrial function during H/R. Collectively, these findings suggest that miR-141 functions as a causative agent in cardiomyocyte injury induced by I/R, primarily by interfering with two mitochondrial regulatory proteins, Sirt1 and MFN2.

Correspondence to: Dr Tao Rui, Division of Cardiology, Department of Medicine, The Affiliated People's Hospital of Jiangsu University, 8 Dianli Road, Zhenjiang, Jiangsu 212002, P.R. China
E-mail: tao_rui8@163.com

Key words: cardiomyocytes, hypoxia/reoxygenation, reactive oxygen species, microRNA-141, sirtuin 1, mitofusin 2

Introduction

Myocardial injury incurred during ischemia is generally attributed to a depletion of myocyte adenosine triphosphate (ATP) production. The reperfusion of the ischemic myocardium is the only recourse to salvaging cardiac function. Paradoxically, reperfusion itself induces further tissue injury. Thus, immense efforts have been expended to gain insight into potential drivers of reperfusion injury, in order to enable the development of therapeutic strategies for the mitigation of reperfusion injury (1,2). To this end, *in vivo* and *ex vivo* models of cardiac ischemia/reperfusion (I/R) have been used. *In vivo* models involve occlusion and the subsequent release of a coronary artery, and tracking cardiac injury and inflammation. This approach more closely simulates the clinical situation; however, due to input from various resident (myocytes, fibroblasts, endothelial cells) and infiltrating immune (neutrophils, monocytes) cells, unravelling the cellular mechanisms is challenging (3). Frequently, cell-based models are used, involving the challenge of cardiomyocytes with hypoxia/reoxygenation (H/R).

Consensus holds that reactive oxygen species (ROS) play a critical role in reperfusion-induced cardiac injury (4-6). Whereas there are several potential sources of ROS in cardiomyocytes, mitochondrial-derived ROS are particularly attractive targets. Mitochondria most likely generate ROS during the normal course of oxidative phosphorylation. The rapid transfer of electrons along the electron transport chain (ETC) can result in the 'leakage' of electrons that can interact with O_2 to form superoxide. A particularly devastating feature of mitochondrial ROS production is the feed-forward mechanism by which ROS-induced ROS release spreads from one mitochondrion to another, ultimately resulting in myocyte dysfunction and death (7,8).

Regulatory mechanisms are operative, to limit excessive cellular ROS levels and associated sequelae. At the transcriptional level, ROS can transactivate genes encoding enzymatic and non-enzymatic antioxidants (4,5). At the translational level, an additional layer of regulation is achieved by microRNAs (miRNAs/miRs) (9-11). miRNAs are non-coding RNAs that

can modulate genetic output of antioxidants, primarily by transcriptional silencing. Members of the miR-200 family (miR-200a, miR-200b, miR-200c, miR-141 and miR-429) can respond to and regulate cellular ROS levels (9,10). Two members of this family, miR-200c and miR-141, have been implicated in various pathologies associated with excessive oxidant stress and mitochondrial dysfunction within the heart, including aging and diabetes (11,12). While an increase in miR-200c driving cardiac I/R or H/R injury has been supported by previous studies (1,2), the role of miR-141 is rather ambiguous (13,14). This is contrary to the available evidence for a ROS/miR-141 pathway being intimately involved in mitochondrial dysfunction (15-17). Thus, in the present study, a reductionist approach was applied to systematically re-examine this issue. The current findings indicate that the challenge of cardiomyocytes with H/R may result in mitochondrial dysfunction via a ROS/miR-141 pathway, in line with a ROS-induced ROS release mechanism.

To address specific targets of miR-141 that may mediate the H/R-induced mitochondrial dysfunction, the present study focused on sirtuin-1 (Sirt1) and mitofusin-2 (MFN2). Sirt1 and MFN2 both are intimately involved in mitochondrial function (18-20) and exerts cardioprotective effects in I/R models (18,21). Of note, a Sirt1/MFN2 pathway has been implicated in I/R-induced mitochondrial dysfunction in hepatocytes (22,23). Herein, evidence was provided that both Sirt1 and MFN2 have functional binding sites for miR-141 on their gene transcripts. Additionally, the blockade of miR-141 can prevent the H/R-induced downregulation of Sirt1and MFN2. Collectively, the results of the present study indicate that the ROS/miR-141/Sirt1/MFN2 pathway may promote myocardial I/R injury by inducing mitochondrial dysfunction.

Materials and methods

Reagents. Mitochondrial ROS was detected using MitoSOX (cat. no. M36008; Thermo Fisher Scientific, Inc.) and Mito-Tempo (cat. no. 1334850995; MilliporeSigma) was used to quench mitochondrial ROS. Mitochondrial membrane potential was assessed using JC-1 (cat. no. 40705ES03; Shanghai Yeasen Biotechnology Co., Ltd.).

For reverse transcription-quantitative PCR (RT-qPCR), the primers used for miRNA were 5'-TAGCCTGCTGGGGTG GAA-3' (forward), and 5'-TATGGTTTTGACGACTGTGTG AT-3' (reverse). The control primers (U6) were 5'-CGCGCT TCGGCAGCACATATACT-3' (forward) and 5'-ACGCTT CACGAATTTGCGTGTC-3' (reverse).

For western blotting, the primary antibodies used were as follows: MFN2 (1:1,000; cat. no. sc-515647; Santa Cruz Biotechnology, Inc.), Sirt1 (1:1,000; cat. no. sc-74465; Santa Cruz Biotechnology, Inc.), and β-actin (1:5,000; cat. no. 66009-1-Ig; ProteinTech Group, Inc.). A horseradish peroxidase-conjugated goat anti-mouse secondary antibody (1:2,000; cat. no. ab205719; Abcam) was used for detection.

siRNA transfection. For RNA interference, two approaches were followed: Small interfering RNA (siRNA) and miRNA. siRNA-Sirt1, as well as a miR-141-3p (miR-141) mimic and an inhibitor were synthesized by Shanghai GenePharma Co., Ltd. The target sequence for Sirt1 siRNA was 5'-CCCUGU AAAGCUUUCAGAA-3' and that of the negative control was 5'-TTCTCCGAACGTGTCACGT-3'. The sequence of miR-141 mimic was 5'-UAACACUGUCUGGUAAAG AUGG-3' and that of the negative control was 5'-UUCUCC GAACGUGUCACGUTT-3'. The sequence of the miR-141 inhibitor was 5'-CCAUCUUUACCAGACAGUGUUA-3' and that of the negative control was 5'-CAGUACUUUUGUGUA GUACAA-3'. All the siRNAs and miRNA mimics/inhibitors were transfected into the HL-1 cells (described below) using Lipofectamine 2000 reagent (cat. no. 11668019; Thermo Fisher Scientific, Inc.). Briefly, two sterilized Eppendorf tubes were prepared for each group of cells. Each tube was filled with 100 μl Opti-MEM (Thermo Fisher Scientific, Inc.). One tube was filled with 5 μl Lipofectamine 2000, whereas the other was filled with 100 pmol mimics/inhibitors/negative control or with 75 pmol siRNAs/negative controls. The two tubes were then evenly mixed and incubated at room temperature for 20 min. The cells transfected with siRNA/mimics/inhibitors were incubated in a standard incubator at 37˚C and 5% CO_2 for 48 h before subsequent experiments.

Hypoxia/reoxygenation (H/R) of HL-1 cells. The HL-1 immortalized murine cardiomyocyte cell line (cat. no. SCC065; Merck KGaA) was grown in DMEM (cat. no. 11995065; Gibco; Thermo Fisher Scientific, Inc.) with 10% FBS (cat. no. 16140071; Gibco; Thermo Fisher Scientific, Inc.) and 1% penicillin/streptomycin (cat. no. 10378016; Gibco; Thermo Fisher Scientific, Inc.) at 37˚C in a standard humidified incubator (95% air/5% CO_2). The H9c2 cell line was obtained from the American Type Culture Collection (cat. no. CRL-1446) and cultured in DMEM containing 10% FBS at 37˚C with 5% CO_2. To induce hypoxia, the culture medium was changed to serum- and glucose-free DMEM, placed into an anaerobic chamber, wherein O_2 was purged with AnaeroPack (Mitsubishi Gas Chemical Co., Inc.) for 3 h (<0.1% O_2, >15% CO_2). Subsequently, the cells were reoxygenated through replenishment with fresh DMEM and rapidly transferred back to the standard incubator. Cell and mitochondrial functions were evaluated at the indicated time points (6 and 12 h) following reoxygenation. As a control, HL-1 cardiomyocytes were incubated with serum- and glucose-free DMEM for 3 h under standard normoxic (20% O_2) conditions at 37˚C with 5% CO_2. and then replenished with fresh DMEM and cultured in normal conditions [normoxia/reoxygenation (N/R)].

Cell injury assays. Cell viability was assessed using four approaches. A Cell Counting Kit-8 assay (CCK-8; cat. no. C0038; Beyotime Institute of Biotechnology) was applied for the detection of metabolic dysfunction of live cells. Cell supernatants were evaluated for the presence of WST-8 formazan produced by dehydrogenase activity of live cells. After incubation for 2 h at 37˚C, the optical density values were detected at 450 nm. Cell apoptosis was measured using an Annexin-V/propidium iodide apoptosis detection kit (cat. no. 640914; BioLegend, Inc.). In brief, cells labelled with FITC-labelled Annexin-V, excluding propidium iodide, were quantified using flow cytometry. Flow cytometric analyses were performed using BD LSRFortessa X-20 (BD Biosciences). Flow cytometry data were analyzed by FlowJo V10 (FlowJo, LLC). As an index of cell membrane disruption, the lactate

dehydrogenase (LDH) content in the cell supernatants was measured using an LDH assay kit (cat. no. A0202; Nanjing Jiancheng Bioengineering Institute). In addition, the creatine kinase-MB (CK-MB) levels in the cell supernatants were measured spectrophotometrically using standard enzyme-linked immunosorbent assay kits (cat. nos. F3500-A and F2801-B; FANKEL Industrial Co., Ltd.) and a microplate reader (800 TS; BioTek Instruments, Inc.) according to the manufacturer's instructions.

Measurement of mitochondrial ROS production. Mitochondrial ROS production was detected using MitoSOX (cat. no. M36008; Thermo Fisher Scientific, Inc.), a cationic cell-permeable probe that enters the mitochondria, is oxidized by superoxide, and fluoresces when bound to nucleotides (e.g., DNA). Cell fluorescence was assessed using a confocal scanning microscope (LSM800; Zeiss AG). The superoxide dismutase (SOD) mimetic, Mito-Tempo (cat. no. 1334850995; MilliporeSigma) was used to quench mitochondrial ROS. ImageJ software (v1.8.0; National Institutes of Health) was used to quantify the fluorescence intensity.

Measurement of mitochondrial membrane potential. The fluorescent probe, JC-1 (cat. no. 40705ES03; Shanghai Yeasen Biotechnology Co., Ltd.), accumulates in the mitochondria and exhibits a red-to-green shift in emission, which is inversely proportional to membrane polarization. The red/green fluorescence intensity ratio of the HL-1 cells was assessed using a confocal scanning microscope (LSM800). ImageJ software (v1.8.0) was used to quantify the fluorescence intensity.

Determination of mitochondrial function. The mitochondrial oxygen consumption rate (OCR) of the HL-1 cells was assessed using an extracellular flux analysis using Seahorse XF Cell Mito Stress kits (Agilent Technologies, Inc.). The OCR of the HL-1 cells ($1x10^4$ cells/well) under various conditions (e.g., ETC inhibitors) was quantified in a Seahorse XFp analyzer using accompanying software (Seahorse Bioscience; Agilent Technologies, Inc.). Various compounds were used to alter mitochondrial ETC function at 37˚C: oligomycin (1 μM, 27 min) to inhibit complex V, carbonyl cyanide-p-trifluoromethoxyphenylhydrazone (1 μM, 27 min) to uncouple oxidative phosphorylation, and a combination of antimycin A/rotenone (1 μM/100 nM, 27 min) to inhibit complexes I/III.

Transmission electron microscopy. The HL-1 cells were prefixed in 2.5% glutaraldehyde (cat. no. P1126; Beijing Solarbio Science & Technology Co., Ltd.) overnight at 4˚C, washed with 0.1 M sodium cacodylate buffer (cat. no. 20840; Sigma-Aldrich; Merck KgaA) and then fixed in 1% osmium tetroxide (cat. no. 18459; Ted Pella, Inc.) for 24 h at 4˚C. The cells were then washed with 0.1 M sodium cacodylate buffer again, dehydrated in an ethanol series, infiltrated with PolyBed epoxy resin (cat. no. GP2001; Wuhan Servicebio Technology Co., Ltd.) and stained with 2% uranyl acetate (Wuhan Servicebio Technology Co., Ltd.) for 10 min and lead citrate (Wuhan Servicebio Technology Co., Ltd.) for 5 min at room temperature. Ultrathin sections were observed under a transmission electron microscope (HT7800; Hitachi, Ltd.). The extent of mitochondrial and cellular pathology was scored using a modification of previously published paradigms (24,25), with 0 assigned to intact mitochondria and 3 to severely damaged mitochondria (Table SI).

Dual luciferase assay. miRanda (http://www.bioinformatics.com.cn/local_miranda_miRNA _target_prediction_120), Tarbase (http://microrna.gr/tarbase/) and TargetScan (www.targetscan.org/vert_72/) were used to predict target genes of miR-141. MFN2 and Sirt1 were identified as potential target genes. The wild-type 3'-UTR and the miR-141 'seed' mutant 3'-UTR of MFN2 and Sirt1 were synthesized *in vitro* and cloned into the psi-CHECK2 (Hanbio Biotechnology Co., Ltd.). luciferase reporter plasmid. 293T cells (cat. no. 12022001; MilliporeSigma). were transfected with psi-CHECK-2 plasmid containing wild-type or mutant derivatives, along with the miRNA control or miR-141 mimic using Lipofectamine 2000. After 24 h, the cells were harvested, lysed, and the ratio of Firefly luciferase to *Renilla* luciferase was assessed. The luciferase activity was detected using the Dual Luciferase Reporter Assay kit (Promega Corp.). The psi-Check2 vector was used for the dual luciferase assay. In this vector, the promoter of Firefly luciferase (Fluc) is sv40, and the promoter of *Renilla*-luciferase (Rluc) is HSV-TK. The binding site region were constructed in the 3'UTR region of Fluc.

RT-qPCR. Total RNA, including miRNA, was extracted from the cultured cells by using Trizol reagent (cat. no. B511311; Sangon Biotech Co., Ltd.). The target miRNA was reverse transcribed into cDNA using the miRNA 1st Strand cDNA synthesis kit (cat. no. MR101-01; Vazyme Biotech Co. Ltd.). The miRNA expression level was determined with a miRNA Universal SYBR qPCR master mix (cat. no. MQ101-01; Vazyme Biotech Co. Ltd.) using the CFX96 Touch Real-Time PCR Detection System (Bio-Rad Laboratories, Inc.). The cycling conditions are listed as follows: Pre-denaturation at 95˚C for 5 min, followed by 40 cycles at 95˚C for 10 sec and 60˚C for 30 sec, and elongation at 95˚C for 15 sec and 60˚C for 60 sec. The relative fold expression of the target, normalized to the corresponding control, was calculated by the comparative $2^{-\Delta\Delta Cq}$ method (26).

Western blotting. HL-1 cells were lysed with ice-cold RIPA lysis buffer (cat. no. P0013E; Beyotime Institute of Biotechnology). BCA protein assay kit (cat. no. P0012; Beyotime Institute of Biotechnology) was used for protein quantification. Equal amounts of protein (20 μg) from each sample were separated using 10% SDS-PAGE and subsequently electro-transferred on to nitrocellulose membranes (cat. no. FFN08; Beyotime Institute of Biotechnology). Following blocking with 5% skim milk powder in 1X Tris-buffered saline containing 0.1% Tween-20 for 2 h at room temperature, the blots were probed with primary antibodies (as aforementioned) overnight at 4˚C. Subsequently, the membrane was incubated with horseradish peroxidase-conjugated secondary antibody (as aforementioned) for 1 h at 37˚C. The immunoreactive proteins were visualized using enhanced chemiluminescence reagent kit (cat. no. P0018M; Beyotime Institute of Biotechnology)and analyzed using ImageJ software (v1.8.0). β-actin served as the loading control to normalize relative protein expression levels.

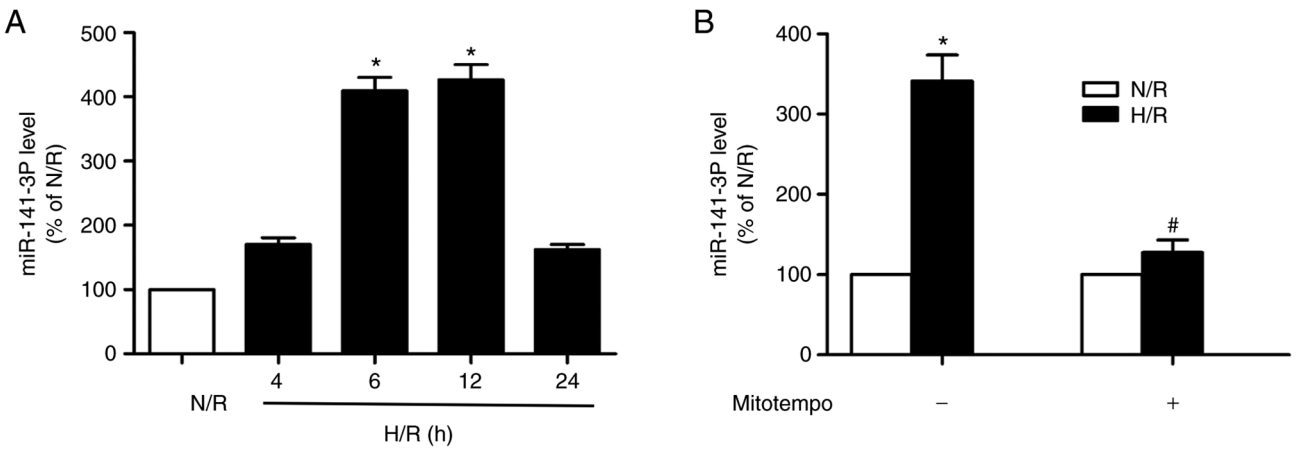

Figure 1. H/R increases miR-141 expression in cardiomyocytes. HL-1 cardiomyocytes were challenged with hypoxia for 3 h and subsequently reoxygenated (H/R). Cells maintained under normoxic conditions for relevant durations served as controls (N/R). Cellular levels of miR-141 were measured using reverse transcription-quantitative PCR. (A) Effect of duration of reoxygenation on miR-141 levels. (B) Effects of a SOD mimetic (Mitotempo), targeting mitochondrial superoxide on miR-141 levels assessed at 6 h following reoxygenation. The cardiomyocytes were pretreated with 20 μM of Mitotempo for 1 h, prior to a challenge with H/R or N/R. Results are presented as the mean ± SEM; n=3. *P<0.01 vs. N/R; $^{\#}$P<0.01 vs. H/R without Mitotempo. H/R, hypoxia/reoxygenation; N/R, normoxia/reoxygenation; SOD, superoxide dismutase; SEM, standard error of the mean.

Statistical analysis. Data are presented as the mean ± standard error of the mean (SEM). An unpaired Student's t-test was performed for direct two-group comparisons and one-way ANOVA was performed for multiple group comparisons followed by the Bonferroni test when ANOVA found a significant F-value and there was no variance in homogeneity; otherwise, Tamhane's T2 post hoc test was used. All statistical analyses were performed using SPSS 13.0 statistical software (SPSS, Inc.). P<0.05 was considered to indicate a statistically significant difference.

Results

H/R increases miR-141-3p expression in HL-1 and H9c2 cardiomyocytes and this event is prevented by quenching mitochondrial superoxide. The challenge of HL-1 cardiomyocytes with H/R increased miR-141 expression within 6 h following reoxygenation. The increment in expression remained elevated at 12 h following reoxygenation and returned to control (normoxia) levels by 24 h (Fig. 1A). Mitochondrial superoxide production is implicated in the I/R-induced myocardial injury (4-6). Thus, a SOD mimetic (Mitotempo) targeting the mitochondria, was used to address the role of mitochondrial ROS in the upregulation of miR-141 expression induced by H/R challenge of the cardiomyocytes. As depicted in Fig. 1B, the SOD mimetic prevented the increase in miR-141 expression at 6 h following reoxygenation. In addition, similar results were observed in H9c2 cells (Fig. S1).

miR-141-3p modulates cardiomyocyte viability following H/R. As shown in Fig. 2 (for HL-1 cells), Fig. S2 (for HL-1 cells) and Fig. S3 (for H9c2 cells), gain- and loss-of-function approaches (miR-141 mimic and inhibitor, respectively) were used to systematically evaluate the role of miR-141 in cardiomyocyte viability following H/R. Firstly, the dehydrogenase activity of live cells was measured, using a CCK-8 assay. As depicted in Figs. 2A and S3A, H/R impaired this index of cell activity. The miR-141 mimic exacerbated the effects of H/R, while the miR-141 inhibitor exerted protective effects. For the N/R of the challenged cells, the miR-141 mimic impaired cell activity, while the miR-141 inhibitor exerted protective effects. Subsequently, using differential Annexin-V/propidium iodide staining, the apoptotic cells were detected. H/R increased the number of cells in early apoptosis; this effect was exacerbated by miR-141 mimic and ameliorated by miR-141 inhibitor (Figs. 2B and S2). Late apoptotic or necrotic cells were also detected following H/R, as indicated by LDH (Figs. 2C and S3B) and CK-MB (Figs. 2D and S3C) release into the supernatants. miR-141 mimic exacerbated the effects of H/R, while miR-141 inhibitor exerted protective effects (Figs. 2C and D, and S3B and C). Establishment of the miR-141 mimic and inhibitor models was shown in Fig. S4.

miR-141-3p modulates the mitochondrial cardiomyocyte OCR induced by H/R. A metabolic flux analysis was performed to assess the mitochondrial function of cardiomyocytes challenged with H/R. Specifically, the OCR of the HL-1 cells was measured during the pharmacological modulation of the mitochondrial ETC. The challenge of the cardiomyocytes with H/R reduced their basal OCR; the miR-141 mimic exacerbated (Fig. 3A), while the inhibitor ameliorated (Fig. 3C) the decrement of basal OCR. The inhibition of ATP synthase with oligomycin revealed the ATP-linked OCR of HL-1 cells. The OCR attributed to mitochondrial ATP production was reduced in cells subjected to H/R; the miR-141 mimic exacerbated (Fig. 3B), while the miR-141 inhibitor (Fig. 3D) blunted the decrement in ATP-coupled OCR.

miR-141-3p modulates mitochondrial superoxide production, membrane potential and damage induced by H/R. The scanning confocal microscopy of the HL-1 cells was used to monitor fluorescent markers of mitochondrial superoxide (mitoSOX) and membrane potential (JC-1). Upon the reoxygenation of hypoxic cardiomyocytes, there was an increase in mitochondrial superoxide production; miR-141 mimic exacerbated, while the miR-141 inhibitor prevented the H/R-induced

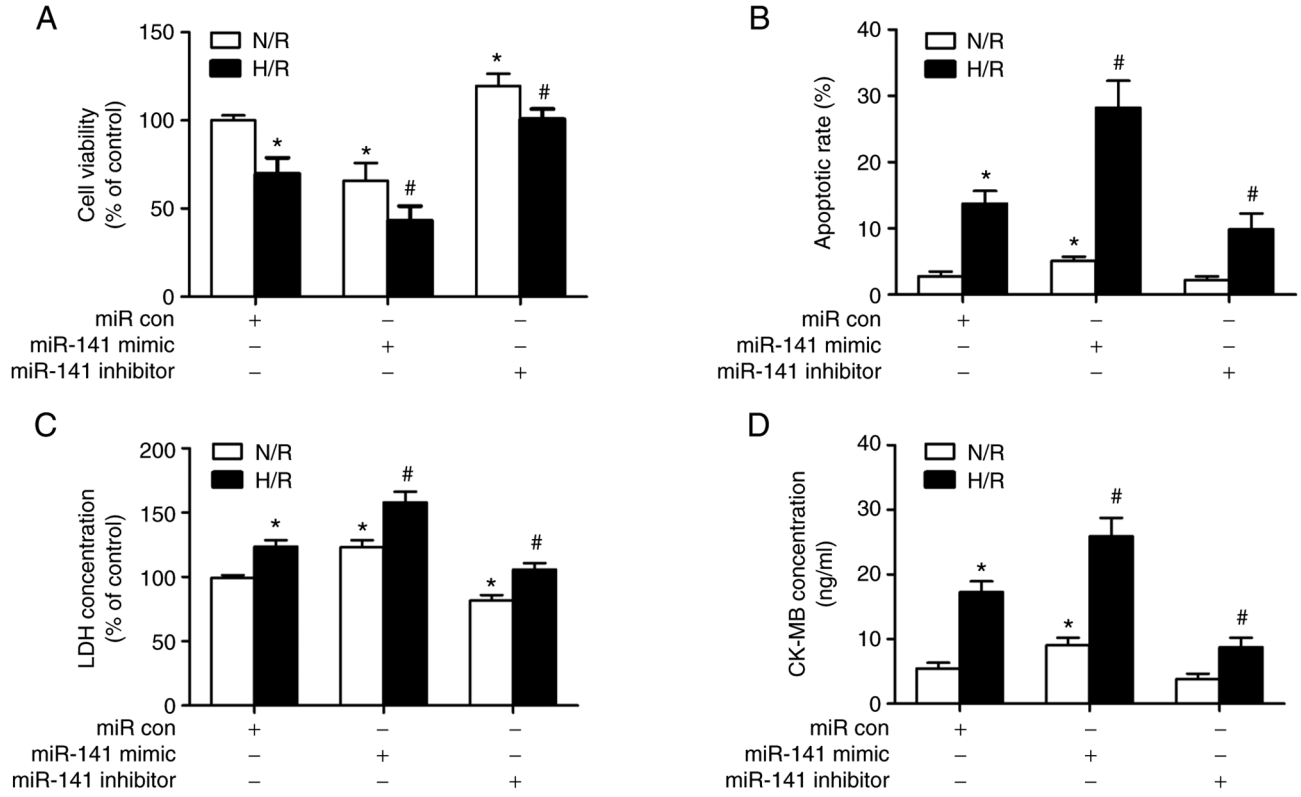

Figure 2. Role of miR-141 in H/R-induced cardiomyocyte viability and death. HL-1 cardiomyocytes were transfected with a miR-141 mimic, miR-141 inhibitor, or their negative controls (miR con). Subsequently, the cells were challenged with H/R and 12 h following reoxygenation and indices of viability, apoptosis and plasma membrane disruption were assessed. (A) The viability of cells was assessed using a CCK-8 assay. (B) Cell apoptosis was assessed using the FACS analysis of Annexin-V/propidium iodide (please see Fig. S1 for quadrant depictions). (C and D) LDH and CK-MB release from cells with ruptured membranes. Results are presented as the mean ± SEM; n=3. *P<0.05 vs. N/R + miR con, #P<0.05 vs. H/R + miR con. H/R, hypoxia/reoxygenation; CCK-8, cell counting kit-8 assay; LDH, lactate dehydrogenase; CK-MB, creatine kinase-MB; SEM, standard error of the mean; miR con, miR control.

generation of superoxide (Fig. 4A and B). The challenge of the HL-1 cells with H/R depolarized the mitochondrial membrane; miR-141 mimic exacerbated, while the inhibitor prevented membrane depolarization (Fig. 4C and D).

Mitochondrial morphology was examined using electron microscopy (Fig. 4E-H) and the results were quantified (Fig. 4I). The normoxic HL-1 cells exhibited discernable mitochondrial membranes and cristae (Fig. 4E). The mitochondria of cells subjected to H/R exhibited signs of structural derangement; they appeared swollen and many lacked defined cristae (Fig. 4F). The miR-141 mimic aggravated the H/R-induced mitochondrial damage, additionally resulting in cell lysis in some cases (Fig. 4G). By contrast, the miR-141 inhibitor partially protected the cells from H/R-induced mitochondrial injury (Fig. 4H).

Sirt1 and MFN2 mRNA are targets of miR-141. Sirt1 and MFN2 have been reported to be depleted in hepatocytes challenged with H/R (22). miRNA target predictor programs (miRanda, Tarbase and TargetScan) identified putative binding sites for miR-141, concurrently on Sirt1 and MFN2 transcripts. To determine whether miR-141 is able to bind to either the 3'-UTR of Sirt1 or MFN2, a luciferase assay was performed. As demonstrated in Fig. 5A and B, co-transfection with miR-141 mimic decreased the relative (Firefly/*Renilla*) luciferase activity of 293T cells transfected with the 3'-UTR of Sirt1 or MFN2, which was not observed in the control sample. According to the binding data, the transfection of HL-1 cells with the miR-141 mimic but not with the miR control, simultaneously decreased Sirt1 and MFN2 protein expression (Fig. 5C and D). Collectively, these findings indicate that miR-141 can bind to the 3'-UTRs of both Sirt1 and MFN2, and decrease their cellular protein levels.

miR-141 inhibitor prevents the H/R-induced downregulation of Sirt1 and MFN2 in HL-1 cells. The H/R challenge of cardiomyocytes decreased their expression of Sirt1 and MFN2 protein (Fig. 6A and B). The miR-141 inhibitor prevented the H/R-induced downregulation of Sirt1 and MFN2. As shown in Fig. S5, Sirt1 siRNA effectively inhibited the expression of Sirt1 in HL-1 cardiomyocytes. Furthermore, transfection of the HL-1 cells with siRNA against Sirt1 reversed the promoting effects of miR-141 inhibitor on MFN2 protein expression (Fig. 6B). The latter observation is consistent with MFN2 being a downstream target of Sirt1 (22,23).

Sirt1 siRNA reverses the protective effects of miR-141 inhibitor on H/R-induced mitochondrial superoxide production and membrane potential. As anticipated, the challenge of cardiomyocytes with H/R increased mitochondrial superoxide production (Fig. 7); an effect significantly prevented by the miR-141 inhibitor. Moreover, Sirt1 siRNA abolished the protective effect of the miR-141 inhibitor, and exacerbated the H/R-induced mitochondrial superoxide production compared with in the H/R + mir-141-inhibitor + control siRNA group.

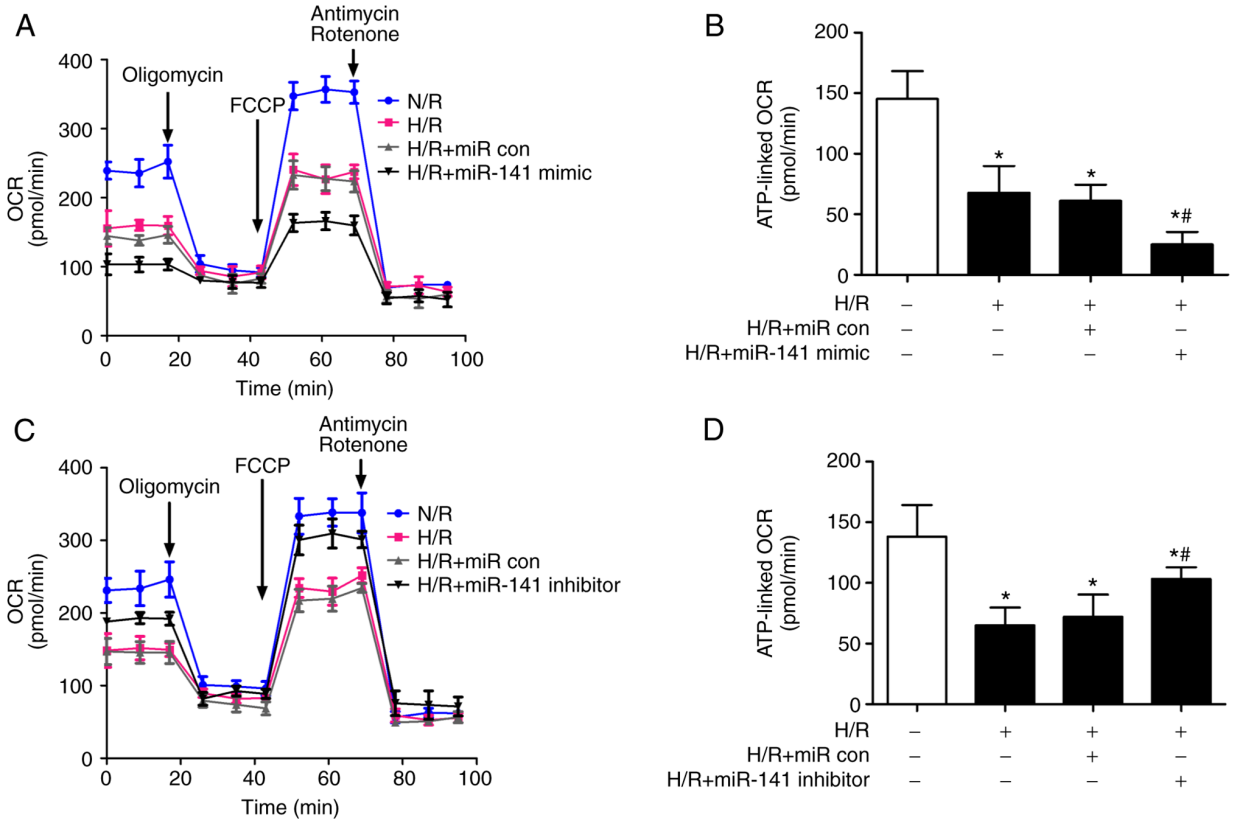

Figure 3. Role of miR-141 in H/R-induced mitochondrial dysfunction of cardiomyocytes. HL-1 cardiomyocytes were transfected with a miR-141 mimic, miR-141 inhibitor, or their negative controls (miR con). Subsequently, the cells were challenged with H/R and 12 h and OCR was evaluated by extracellular flux analysis. In brief, after the baseline OCR was obtained, oligomycin (1 μM, 27 min) was added to obtain ATP-coupled OCR (baseline-oligomycin). Subsequently, carbonyl cyanide-p-trifluoromethoxyphenylhydrazone (1 μM, 27 min) was added to uncouple oxidative phosphorylation followed by a combination of antimycin A/rotenone (1 μM/100 nM, 27 min) to inhibit complexes I/III. (A and B) The complete extracellular flux analyses of cardiomyocyte OCR challenged with (A) H/R and miR-141 mimic, and the OCR linked to (B) ATP production. (C and D) The complete extracellular flux analyses of cardiomyocyte OCR challenged with (C) H/R and miR-141 inhibitor, and (D) the OCR linked to ATP production. Bar graphs represent the mean ± SEM; n=3. *P<0.05 vs. normoxic control (open bars), #P<0.05 vs. H/R + miR con. miR con, miR control; H/R, hypoxia/reoxygenation; OCR, reoxygenation mitochondrial oxygen consumption rate; SEM, standard error of the mean.

Similar results were observed concerning the H/R-induced changes in mitochondrial membrane potential. The challenge of cardiomyocytes with H/R depolarized the mitochondrial membrane (Fig. 8), an effect which was attenuated by miR-141 inhibitor. Additionally, Sirt1 siRNA abolished the protective effects of the miR-141 inhibitor, and also exacerbated the H/R-induced depolarization of the mitochondrial membrane.

Discussion

I/R-induced myocardial dysfunction and injury are attributed to enhanced ROS production by cardiomyocytes, a major source of ROS being the ETC of mitochondria (4-8). The initial overproduction of ROS generates a self-amplifying wave of oxidant stress along the ETC that leads to mitochondrial dysfunction and culminates in cardiomyocyte death and tissue necrosis (5,7,8). Transcriptional regulatory mechanisms exist to limit cellular oxidative stress and associated sequelae; however, the generation of defensive proteins can be negated at the post-transcriptional level by non-coding RNAs, miRNAs. miRNAs exert their effects by binding to complementary mRNA sites, preventing their translation. miR-141, a member of the miR-200 family, can respond to oxidative stress (27) and can induce mitochondrial dysfunction (16) and cell death (13,14). Thus, the main focus of the present study was to elucidate the role of miR-141 in the mitochondrial dysfunction of cardiomyocytes, elicited by an H/R challenge. Three novel findings-to the best of our knowledge-were presented in the current study: i) The H/R-induced decrement in mitochondrial oxygen utilization, increment in ROS production, and membrane depolarization, as well as cardiomyocyte apoptosis is ameliorated by miR-141 inhibitor; ii) miR-141 simultaneously targets Sirt1 and MFN2 mRNA; and iii) the mitochondria-associated protein, MFN2, is a downstream target of Sirt1.

The results of the present study using a cell-based model of simulated I/R are in line with mitochondrial ROS-induced ROS release playing a prominent role in I/R-induced cardiomyopathy (5,7,8). In this scenario, upon the reoxygenation of hypoxic cardiomyocytes (H/R), there is a surge in mitochondrial ROS production, resulting in an increase in inner membrane permeability and the subsequent collapse of the membrane potential. The oxidative stress is propagated from one mitochondrion to another, eventually resulting in cell death. Herein, the H/R challenge of HL-1 or H9c2 cardiomyocytes resulted in an upregulation of miR-141; an event inhibited by a SOD-mimetic that accumulates in mitochondria (Figs. 1 and S1). Furthermore, the H/R-induced mitochondrial

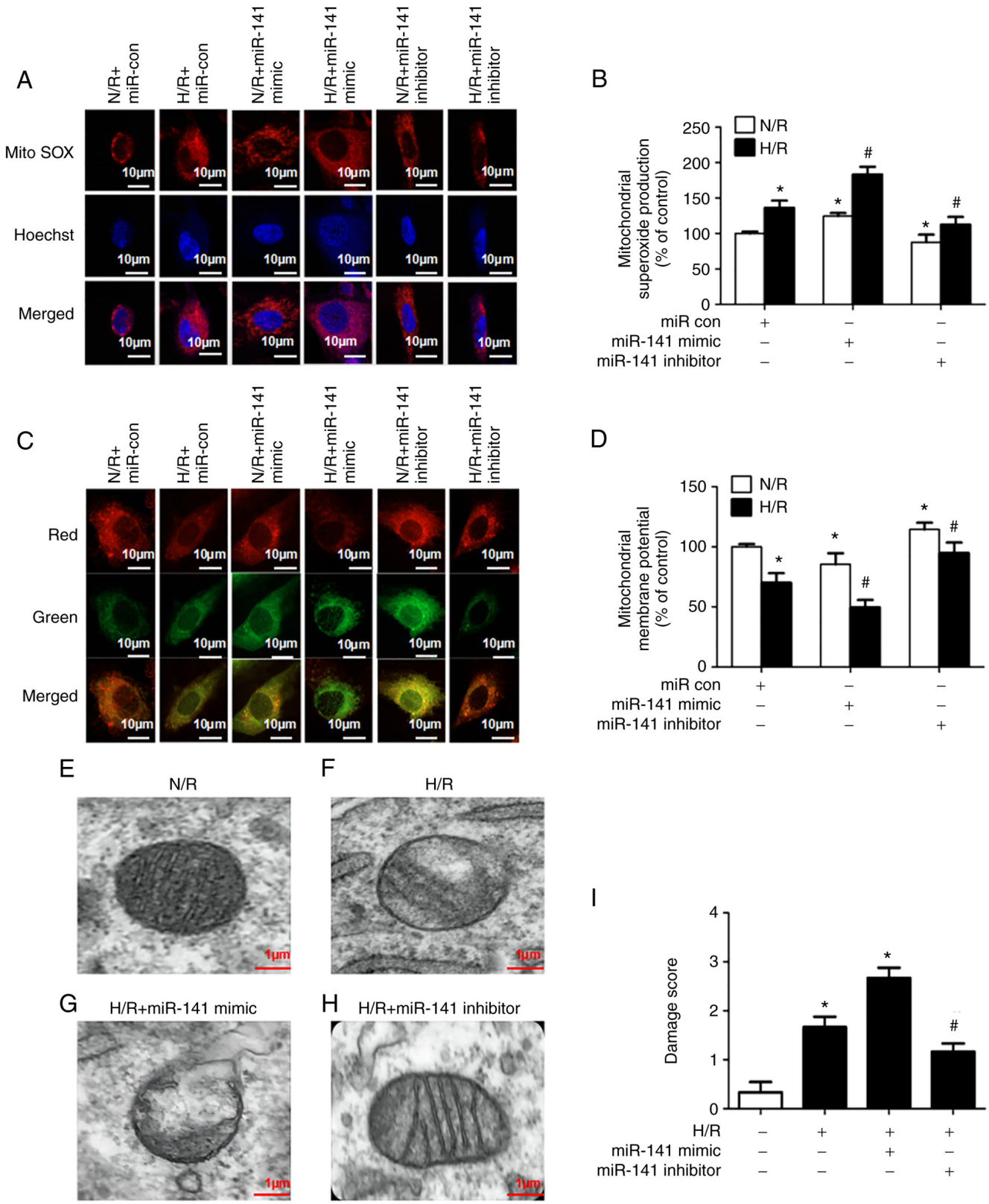

Figure 4. Role of miR-141 in the H/R-induced increase in mitochondrial superoxide production, decrease in mitochondrial membrane potential, and ultrastructural derangements. HL-1 cardiomyocytes were transfected with a miR-141 mimic, miR-141 inhibitor, or their negative controls (miR con). Subsequently, the cells were challenged with H/R. (A and B) Mitochondrial superoxide production was assessed using the fluorescence microscopy of MitoSOX red, 6 h after reoxygenation. An increase in superoxide production is indicated by an increase in intensity of red fluorescence. (A) Representative images and (B) quantification results are presented. (C and D) Mitochondrial membrane potential was assessed using the fluorescence microscopy of JC-1 6 h after reoxygenation. Mitochondrial membrane depolarization is indicated by a shift from red to green fluorescence. (C) Representative images and (D) quantification results are presented. Bar graphs are represent the mean ± SEM; n=3. *P<0.05 vs. control (open bar); #P<0.05 vs. H/R. (E-I) Mitochondrial morphology was assessed using electron microscopy, 12 h after reoxygenation. (E-H) Representative images and in (E-H) and (I) quantification results are presented. The scoring paradigm is presented in Table SI. In brief, a value of 0 was assigned to intact mitochondria and 3 to severely damaged mitochondria. Each bar graph represents scoring of 6 photomicrographs/group by 3 investigators. Bar graphs represent the mean ± SEM. *P<0.05 vs. control (open bar); #P<0.05 vs. H/R. H/R, hypoxia/reoxygenation; miR con, miR control; SEM, standard error of the mean.

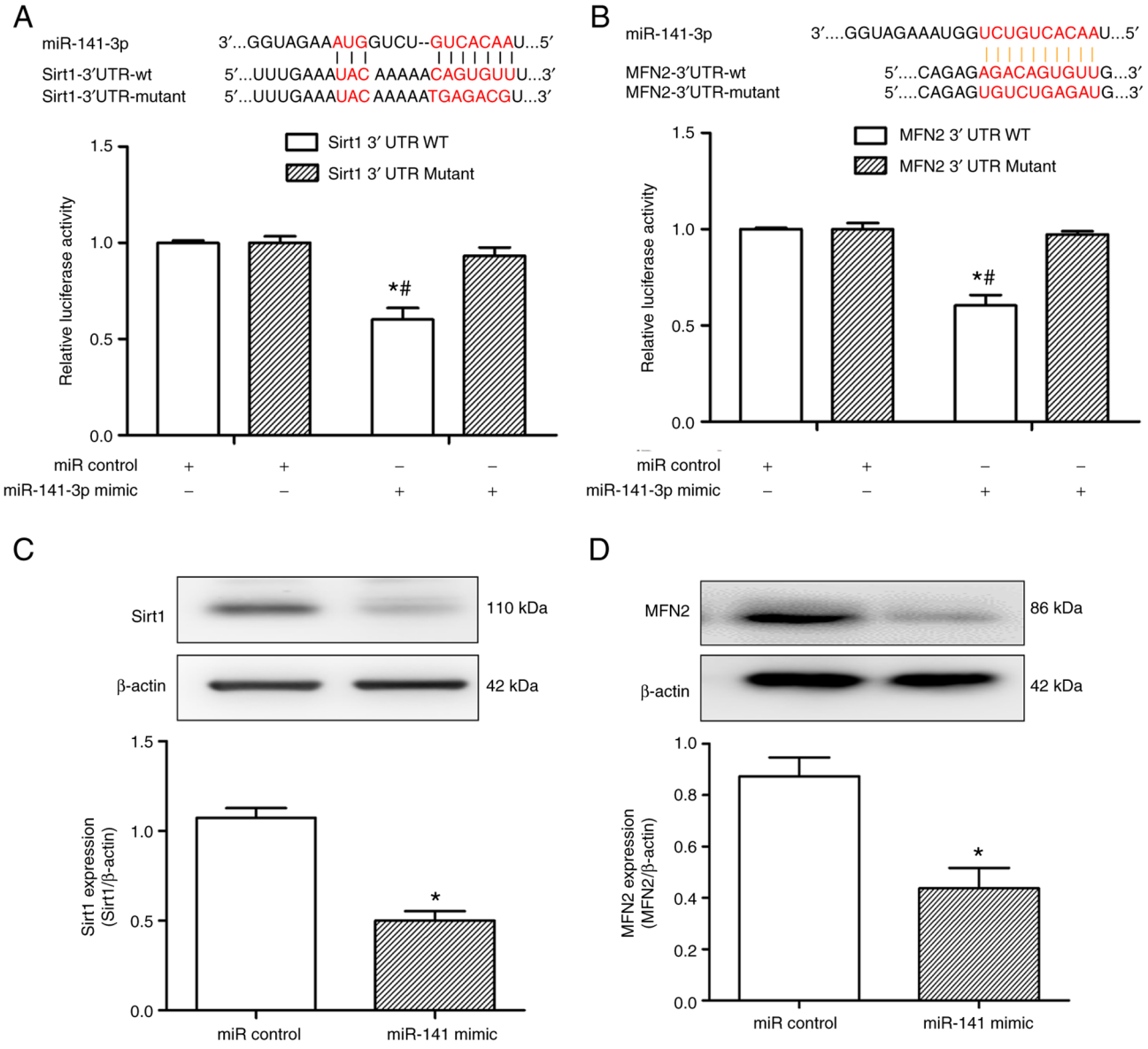

Figure 5. miR-141 inhibits Sirt1 and MFN2 expression in cardiomyocytes. (A and B) Sirt1 and MFN2 contain conserved miR-141-3p interaction motifs within their 3'-UTRs (red font). The sequences of the wild-type and mutant 3'-UTRs of Sirt1 and MFN2 for luciferase reporter assay are also demonstrated. For the luciferase assay, 293T cells were co-transfected with 0.4 μg WT or (A) mutant Sirt1 or (B) MFN2 3'-UTR reporter plasmids in the presence of miR-141-3p mimic (200 nM) or miR control. Luciferase activity was measured after 24 h. The results are quantitated as a ratio of Firefly/*Renilla* luciferase. (C and D) HL-1 cardiomyocytes were transfected with a miR-141 mimic or its negative control (con). (C) Sirt1 and (D) MFN2 protein levels were assessed using western blotting after 24 h. Representative blots are shown in the upper panels and quantification by densitometry in the lower panels. All bar graphs represent the mean ± SEM; n=3. *P<0.05 vs. miR control. $^{\#}$P<0.05 vs. 3'-UTR Mutant. Sirt1, sirtuin-1; MFN2, mitofusin-2; WT, wild-type; con, control; SEM, standard error of the mean.

ROS generation, membrane depolarization, ultrastructural derangements, as well as cardiomyocyte apoptosis were blunted by an inhibitor of miR-141 (Figs. 2, 4, S2 and S3). In addition, miR-141 also impaired the viability of the N/R-treated cells, while miR-141 inhibitor increased cell viability. The possible reason is that miR-141 affects cell viability by regulating the expression of relevant target genes. Collectively, these findings indicated that subjecting cardiomyocytes to simulated I/R increased mitochondrial ROS production, subsequently inducing more mitochondrial ROS production and dysfunction via miR-141.

The specific components of the signaling pathway by which mitochondrial ROS initially promotes expression of miR-141 are not yet entirely clear. However, the tumor suppressor protein, p53, is an attractive candidate. An *in silico* approach indicates that functional p53 motifs are present on the miR-200 family of genes, including miR-141 (28), which can be activated by p53 in response to oxidant stress in hepatocytes (29). Moreover, the cardiomyocyte expression of p53 can be increased by an H/R challenge in a ROS-dependent manner (30). Further studies are required to systematically evaluate the signaling pathway leading to miR-141 expression induced by mitochondrial oxidant stress.

Of note, in the present study, the H/R challenge of HL-1 cardiomyocytes reduced the mitochondrial oxygen consumption associated with ATP production. This defect

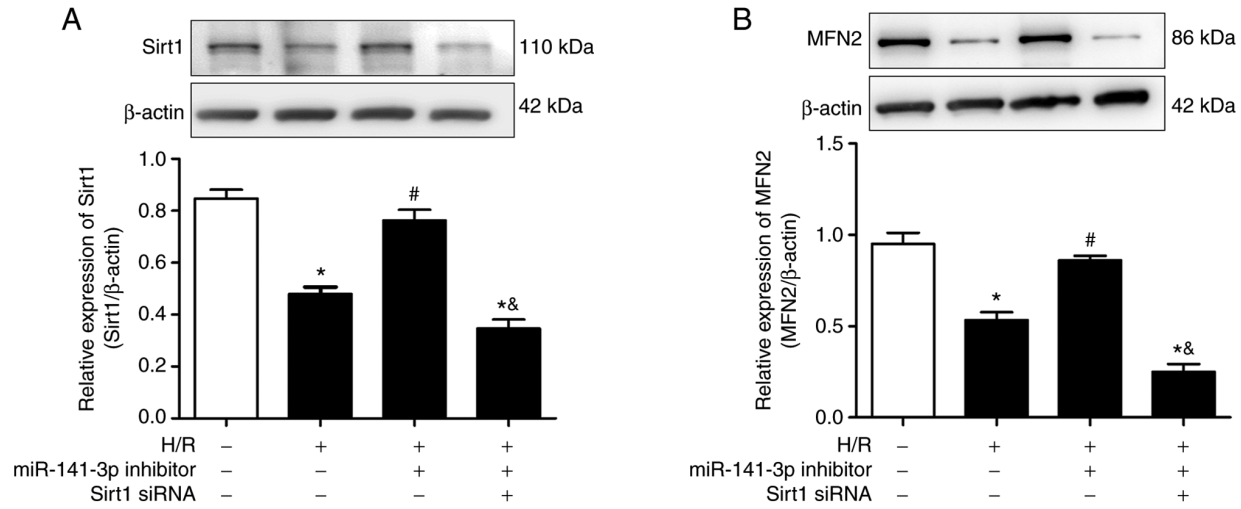

Figure 6. Silencing of Sirt1 negates the rescue of MFN2 by the miR-141 inhibitor after H/R challenge of cardiomyocytes. HL-1 cardiomyocytes were transfected with Sirt1 siRNA and 24 h later some cells were transfected with miR-141 inhibitor for an additional 24 h. Subsequently, all cells were subjected to H/R. Sirt1 (A) and MFN2 (B) protein levels were measured using western blotting 6 h following reoxygenation. Representative blots are depicted in the upper panels and quantification by densitometry in the lower panels. All bar graphs represent the mean ± SEM; n=3. *P<0.01 vs. control (open bars); $^{\#}$P<0.05 vs. H/R, $^{\&}$P<0.01 vs. H/R + miR-141 inhibitor. Sirt1, sirtuin-1; MFN2, mitofusin-2; H/R, hypoxia/reoxygenation; SEM, standard error.

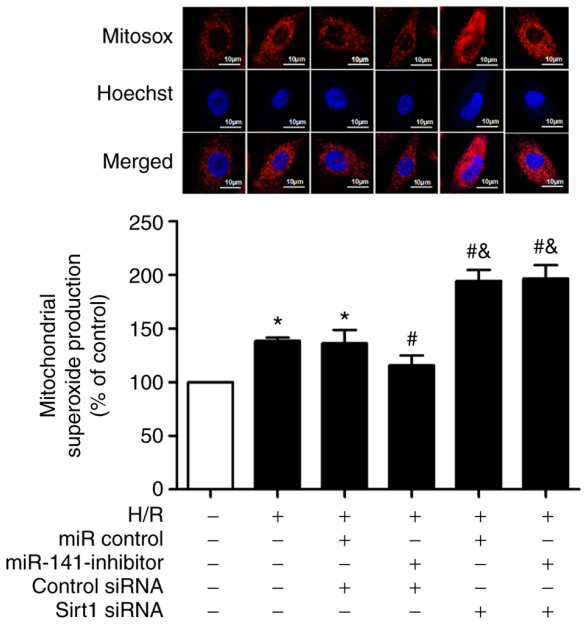

Figure 7. Silencing of Sirt1 negates the damping of mitochondrial superoxide production by miR-141 inhibitor following the H/R challenge of cardiomyocytes. HL-1 cardiomyocytes were transfected with Sirt1 siRNA or control siRNA. Some cells were also transfected 24 h later with miR-141 inhibitor or miR control for an additional 24 h. Subsequently, the cells were subjected to H/R. Mitochondrial superoxide production was evaluated using the fluorescence microscopy of MitoSOX red 12 h following reoxygenation. An increase in superoxide production is indicated by an increase in intensity of red fluorescence. Representative images are shown in the upper panel and quantification below. All bar graphs represent the mean ± SEM; n=3. *P<0.05 vs. control (open bar); $^{\#}$P<0.05 vs. H/R + miR control + control siRNA; $^{\&}$P<0.01 vs. H/R + miR-141 inhibitor + control siRNA. Sirt1, sirtuin-1; H/R, hypoxia/reoxygenation; SEM, standard error of the mean.

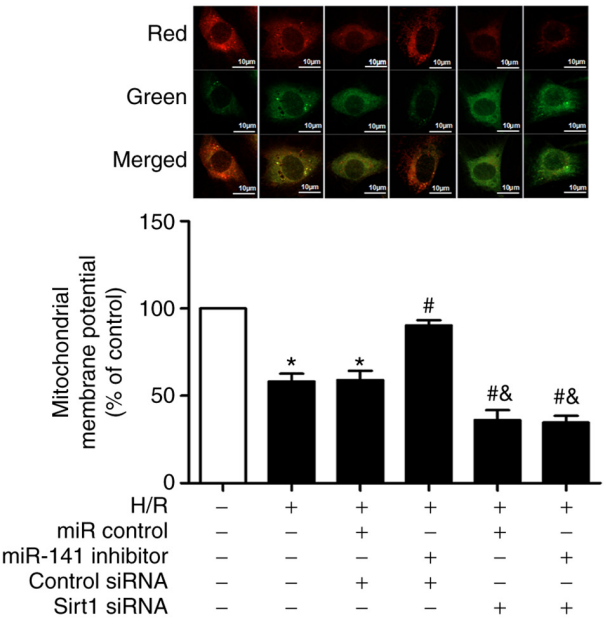

Figure 8. Silencing of Sirt1 negates the rescue of mitochondrial membrane potential by miR-141 inhibitor following the H/R challenge of cardiomyocytes. HL-1 cardiomyocytes were transfected with Sirt1 siRNA or control siRNA. Some cells were also transfected 24 h later with miR-141 inhibitor or miR control for an additional 24 h. Subsequently, the cells were subjected to H/R. Mitochondrial membrane potential was assessed using the fluorescence microscopy of JC-1 12 h following reoxygenation. Mitochondrial membrane depolarization is indicated by a shift from red to green fluorescence. Representative images are shown in the upper panel and quantification in the lower panel. All bar graphs represent the mean ± SEM; n=3. *P<0.05 vs. control (open bar); $^{\#}$P<0.05 vs. H/R + miR control + control siRNA; $^{\&}$P<0.01 vs. H/R + miR-141 inhibitor + control siRNA. Sirt1, sirtuin-1; H/R, hypoxia/reoxygenation; SEM, standard error of the mean.

in oxidative phosphorylation was exaggerated by a miR-141 mimic (Fig. 3A and B), but was attenuated by a miR-141 inhibitor (Fig. 3C and D). These findings are in accordance with those of a previous study implicating a role for miR-141 in mitochondrial oxidative phosphorylation (16). Specifically, miR-141 targets Slc25a3, a mitochondrial phosphate carrier. The Slc25a3 carrier is important for the delivery of inorganic phosphate to the mitochondrial matrix for the

generation of ATP from ADP. The overexpression of miR-141 in HL-1 cardiomyocytes reduces Slc25a3 and cellular ATP production (16). Thus, a potential mechanism by which miR-141 decreased ATP-linked oxygen uptake in the present study may be by limiting inorganic phosphate availability for ATP production.

Sirt1 is a cardioprotective protein that promotes redox homeostasis during oxidant stress among other beneficial effects, which are exerted through the deacetylation of proteins with antioxidant activities, including FOXO, and PGC-1α (18,31,32). Notably, PGC1α is a critical regulator of mitochondrial function through activation of mitochondrial biogenesis and energy metabolism (30). Specifically, Sirt1 can ameliorate cardiomyocyte apoptosis and ROS production (18). Furthermore, the induction of Sirt1 reduces cardiomyocyte dysfunction induced by I/R or H/R (30,33). Of note, miR-141 is expression increased and targets Sirt1 in a cell-based model of Parkinson's disease, involving the challenge of neuron-like cells with a toxin that disrupts the mitochondrial ETC and resulting in cellular oxidant stress and death (15,17). Additional evidence in support of the role of Sirt1 in maintaining mitochondrial hemostasis during oxidative stress is provided by the results of the present study. In brief, miR-141 regulates the impact of H/R on mitochondrial structure (Fig. 4E-H) and function (Fig. 3), as well as cell viability (Figs. 2 and S3). The miR-141 mimic exacerbated the effects of H/R, while a miR-141 inhibitor was protective. Additionally, Sirt1 was a target of miR-141 and the silencing of Sirt1 negated the regulatory function of miR-141 on H/R-induced mitochondrial ROS production (Fig. 7) and membrane collapse (Fig. 8).

MFN2 is an outer mitochondrial membrane GTPase that has been implicated in optimal mitochondrial functioning (20). As depicted in Fig. 6, MFN2 is a target of Sirt1. Previous studies have indicated that MFN2 levels decrease after H/R, and either stabilizing or enhancing MFN2 levels protects cells from H/R (21-23). The protective effect of MFN2 has been attributed to either the fusion-induced optimization of mitochondrial oxidative phosphorylation (21) or the induction of mitophagy to remove defective mitochondria (22,23). Irrespectively, both events serve to maintain a cellular pool of optimally functioning mitochondria. In fact, MFN2 maintains mitochondrial homeostasis in cardiomyocytes via both fusion events and mitophagy (34). Of note, the deacetylation of MFN2 by Sirt1 is protective against hepatic I/R or hepatocyte H/R (22,23). Specifically, Sirt1 deacetylates at two lysine residues in the C-terminus of MFN2 leading to autophagy activation (22). In the present study, the Sirt1/MFN2 pathway was operative in cardiomyocyte H/R, with miR-141 targeting both components of this pathway (Fig. 5). This observation provides an explanation for the observation that i) simulated I/R of aged hepatocytes resulted in the loss of both Sirt1 and MFN2; and ii) the co-overexpression of Sirt1 and MFN2, and not the overexpression of either protein alone, mitigated the mitochondrial dysfunction and hepatocyte death induced by H/R (22).

The H/R challenge of cardiomyocytes reduced MFN2 protein levels, an effect mitigated by the silencing of Sirt1 (Fig. 6B). This observation is in accordance with the ability of Sirt1 to promote mitochondrial biogenesis in hepatocytes by induction of the MFN2 gene (35). Whereas the deacetylation of MFN2 by Sirt1 has been previously reported (22), the mechanisms by which Sirt1 regulates MFN2 protein expression remain unclear. Previous research has revealed that PGC-1α is a target protein of Sirt1, and that the overexpression of Sirt1 can cause an increase in PGC-1α protein expression (36). Furthermore, PGC1α can regulate Mfn2 transcription by binding to its promoter region (37). More importantly, the mitochondrial dysfunction induced by an H/R challenge of H9c2 cardiomyocytes is blunted by Sirt1-induced expression of PGC1α (30). Furthermore, PGC1α can stimulate MFN2 mRNA and protein expression in skeletal muscle (38). Briefly, the ability of Sirt1 to induce MFN2 protein expression is not unprecedented, albeit the mechanisms involved have not been systematically assessed. A possible mechanism through which Sirt1 can regulate MFN2 expression is that Sirt1 may regulate MFN2 transcription through its co-transcriptional regulator, PGC1α.

Mitochondria are dynamic organelles that undergo fission and fusion. MFN2 is a well characterized protein driving mitochondrial fusion, while dynamin-related protein 1 (DRP1) is a major regulator of mitochondrial fission (39,40). The H/R-induced mitochondrial ROS production and structural derangements noted in the present study are reminiscent of mitochondrial fission/fragmentation. Of note, a role for the Sirt1/DRP1 pathway in a cell-based model of hyperglycemia to simulate diabetes has been previously reported by the authors. In brief, an H/R challenge of cardiomyocytes pre-conditioned with glucose (30 mM) decreased Sirt1 levels and activated DRP1, thereby promoting mitochondrial fragmentation (41). Thus, it is likely that Sirt1 can modulate mitochondrial dynamics by reciprocal regulation of regulatory proteins, including MFN2 and DRP1.

A major disadvantage is that the total number of miRNAs that can target Sirt1 and MFN2 is expanding. For example, miR-22, -34a, -9, -29c and -92a, as well as miR-141 can target Sirt1 [(17,42-44), and the results of the present study], while miR-195, -106b, -93 and -20b, as well as miR-141 can target MFN2 [(45-47), and the results of the present study]. Specifically, miR-34a, miR-141 and miR-9 may influence Parkinson's disease pathogenic processes by targeting Sirt1 (17). Suppression of miR-34a has been reported to provide anti-apoptotic protection by directly targeting Sirt1 in a myocardial IR injury model (42). Furthermore, miR-92a can prevent the migration of H_2O_2-induced vascular smooth muscle cells by suppressing the expression of Sirt1 (43) and miR-29c suppresses liver tumorigenesis by binding to the 3'-untranslated region of Sirt1 mRNA (44). In addition, miR-195 may impair mitochondrial function by targeting MFN2 in breast cancer cells (45), and miR-106b and miR-93 can control excessive mitophagy and restrain cell death by targeting MFN2 (46). Furthermore, miR-20b promotes cardiac hypertrophy by directly targeting MFN2 (47). Thus, drawing firm conclusions regarding the therapeutic potential of any miRNA is rather difficult. Additionally, the use of a cell-based model of simulated ischemia/reperfusion further complicates the translational applicability. Whereas cell-based models are very useful in uncovering signaling pathways in a given resident cardiac cell (e.g., cardiomyocyte), contributions from other resident or infiltrating cells cannot be considered (3). Nonetheless, miR-141 can target both components of the Sirt1/MFN2 pathway (Fig. 5), which has been implicated in mitochondrial homeostasis during I/R or H/R [(22,23), and the

results of the present study]. The targeting of both components of the Sirt1/MFN2 pathway permits an improved degree of specificity in the modulation of mitochondrial function by miR-141. This intriguing aspect of miR-141 modulation of the Sirt1/MFN2 pathway warrants further investigation with a view toward potential therapeutic application.

In conclusion, the challenge of cardiomyocytes with H/R increases miR-141 expression. miR-141 expression is induced by mitochondrial ROS production and serves to perpetuate the oxidant stress, ultimately leading to cell death. The H/R-induced mitochondrial ROS production and dysfunction are mediated by miR-141, most likely via the targeting of both components of the Sirt1/MFN2 pathway.

Acknowledgements

Not applicable.

Funding

The present study was supported by the National Natural Science Foundation of China (grant no. 82172172) and the Science and Technology Bureau of Zhengjiang (grant no. SH2019048).

Availability of data and materials

The datasets used and/or analyzed during the current study are available from the corresponding author on reasonable request.

Authors' contributions

HZ, HW and TR contributed to the conceptualization and the design of the present study. HZ, RL and HW performed the experiments and analyzed the data. YW, YY, PK and KW were responsible for the acquisition, analysis and interpretation of the data. HZ and PK contributed to the drafting of the manuscript. RL and KW confirm the authenticity of all the raw data. All authors read and approved the final manuscript.

Ethics approval and consent to participate

Not applicable.

Patient consent for publication

Not applicable.

Competing interests

The authors declare that they have no competing interests.

References

1. Heusch G: Myocardial ischaemia-reperfusion injury and cardioprotection in perspective. Nat Rev Cardiol 17: 773-789, 2020.
2. Davidson SM, Adameová A, Barile L, Cabrera-Fuentes HA, Lazou A, Pagliaro P, Stensløkken KO, Garcia-Dorado D and EU-CARDIOPROTECTION COST Action (CA16225): Mitochondrial and mitochondrial-independent pathways of myocardial cell death during ischaemia and reperfusion injury. J Cell Mol Med 24: 3795-3806, 2020.
3. Ren D, Wang X, Ha T, Liu L, Kalbfleisch J, Gao X, Williams D and Li C: SR-A deficiency reduces myocardial ischemia/reperfusion injury; involvement of increased microRNA-125b expression in macrophages. Biochim Biophys Acta 1832: 336-346, 2013.
4. Cadenas S: ROS and redox signaling in myocardial ischemia-reperfusion injury and cardioprotection. Free Radic Biol Med 117: 76-89, 2018.
5. Granger DN and Kvietys PR: Reperfusion injury and reactive oxygen species: The evolution of a concept. Redox Biol 6: 524-551, 2015.
6. Bugger H and Pfeil K: Mitochondrial ROS in myocardial ischemia reperfusion and remodeling. Biochim Biophys Acta Mol Basis Dis 1866: 165768, 2020.
7. Chen YR and Zweier JL: Cardiac mitochondria and reactive oxygen species generation. Circ Res 114: 524-537, 2014.
8. Zorov DB, Juhaszova M and Sollott SJ: Mitochondrial reactive oxygen species (ROS) and ROS-induced ROS release. Physiol Rev 94: 909-950, 2014.
9. Magenta A, Ciarapica R and Capogrossi MC: The emerging role of miR-200 family in cardiovascular diseases. Circ Res 120: 1399-1402, 2017.
10. Kalinina EV, Ivanova-Radkevich VI and Chernov NN: Role of MicroRNAs in the regulation of redox-dependent processes. Biochemistry (Mosc) 84: 1233-1246, 2019.
11. Magenta A, Lorde R, Syed SB, Capogrossi MC, Puca A and Madeddu P: Molecular therapies delaying cardiovascular aging: Disease- or health-oriented approaches. Vasc Biol 2: R45-R58, 2020.
12. Qadir MMF, Klein D, Álvarez-Cubela S, Domínguez-Bendala J and Pastori RL: The role of MicroRNAs in diabetes-related oxidative stress. Int J Mol Sci 20: 5423, 2019.
13. Yao B, Wan X, Zheng X, Zhong T, Hu J, Zhou Y, Qin A, Ma Y and Yin D: Critical roles of microRNA-141-3p and CHD8 in hypoxia/reoxygenation-induced cardiomyocyte apoptosis. Cell Biosci 10: 20, 2020.
14. Qin Q, Cui L, Zhou Z, Zhang Z, Wang Y and Zhou C: Inhibition of microRNA-141-3p reduces hypoxia-induced apoptosis in H9c2 rat cardiomyocytes by activating the RP105-dependent PI3K/AKT signaling pathway. Med Sci Monit 25: 7016-7025, 2019.
15. Zheng Y, Dong L, Liu N, Luo X and He Z: Mir-141-3p regulates apoptosis and mitochondrial membrane potential via targeting sirtuin1 in a 1-methyl-4-phenylpyridinium in vitro model of Parkinson's disease. Biomed Res Int 2020: 7239895, 2020.
16. Baseler WA, Thapa D, Jagannathan R, Dabkowski ER, Croston TL and Hollander JM: miR-141 as a regulator of the mitochondrial phosphate carrier (Slc25a3) in the type 1 diabetic heart. Am J Physiol Cell Physiol 303: C1244-C1251, 2012.
17. Delavar MR, Baghi M, Safaeinejad Z, Kiani-Esfahani A, Ghaedi K and Nasr-Esfahani MH: Differential expression of miR-34a, miR-141, and miR-9 in MPP+-treated differentiated PC12 cells as a model of Parkinson's disease. Gene 662: 54-65, 2018.
18. Zhang J, Ren D, Fedorova J, He Z and Li J: SIRT1/SIRT3 modulates redox homeostasis during ischemia/reperfusion in the aging heart. Antioxidants (Basel) 9: 858, 2020.
19. Lee IH: Mechanisms and disease implications of sirtuin-mediated autophagic regulation. Exp Mol Med 51: 1-11, 2019.
20. Filadi R, Pendin D and Pizzo P: Mitofusin 2: From functions to disease. Cell Death Dis 9: 330, 2018.
21. Olmedo I, Pino G, Riquelme JA, Aranguiz P, Díaz MC, López-Crisosto C, Lavandero S, Donoso P, Pedrozo Z and Sánchez G: Inhibition of the proteasome preserves Mitofusin-2 and mitochondrial integrity, protecting cardiomyocytes during ischemia-reperfusion injury. Biochim Biophys Acta Mol Basis Dis 1866: 165659, 2020.
22. Chun SK, Lee S, Flores-Toro J, Rebecca YU, Yang MJ, Go KL, Biel TG, Miney CE, Louis SP, Law BK, *et al*: Loss of sirtuin 1 and mitofusin 2 contributes to enhanced ischemia/reperfusion injury in aged livers. Aging Cell 17: e12761, 2018.
23. Biel TG, Lee S, Flores-Toro JA, Dean JW, Go KL, Lee MH, Law BK, Law ME, Dunn WA Jr, Zendejas I, *et al*: Sirtuin 1 suppresses mitochondrial dysfunction of ischemic mouse livers in a mitofusin 2-dependent manner. Cell Death Differ 23: 279-290, 2016.
24. Liu Y, Nguyen P, Baris TZ and Poirier MC: Molecular analysis of mitochondrial compromise in rodent cardiomyocytes exposed long term to nucleoside reverse transcriptase inhibitors (NRTIs). Cardiovasc Toxicol 12: 123-134, 2012.

25. Poli G, Guasti D, Rapizzi E, Fucci R, Canu L, Bandini A, Cini N, Bani D, Mannelli M and Luconi M: Morphofunctional effects of mitotane on mitochondria in human adrenocortical cancer cells. Endocr Relat Cancer 20: 537-550, 2013.
26. Livak KJ and Schmittgen TD: Analysis of relative gene expression data using real-time quantitative PCR and the 2(-Delta Delta C(T)) method. Methods 25: 402-408, 2001.
27. Magenta A, Cencioni C, Fasanaro P, Zaccagnini G, Greco S, Sarra-Ferraris G, Antonini A, Martelli F and Capogrossi MC: miR-200c is upregulated by oxidative stress and induces endothelial cell apoptosis and senescence via ZEB1 inhibition. Cell Death Differ 18: 1628-1639, 2011.
28. Tamura M, Sasaki Y, Kobashi K, Takeda K, Nakagaki T, Idogawa M and Tokino T: CRKL oncogene is downregulated by p53 through miR-200s. Cancer Sci 106: 1033-1040, 2015.
29. Xiao Y, Yan W, Lu L, Wang Y, Lu W, Cao Y and Cai W: p38/p53/miR-200a-3p feedback loop promotes oxidative stress-mediated liver cell death. Cell Cycle 14: 1548-1558, 2015.
30. Du JK, Cong BH, Yu Q, Wang H, Wang L, Wang CN, Tang XL, Lu JQ, Zhu XY and Ni X: Upregulation of microRNA-22 contributes to myocardial ischemia-reperfusion injury by interfering with the mitochondrial function. Free Radic Biol Med 96: 406-417, 2016.
31. D'Onofrio N, Servillo L and Balestrieri ML: SIRT1 and SIRT6 signaling pathways in cardiovascular disease protection. Antioxid Redox Signal 28: 711-732, 2018.
32. Elibol B and Kilic U: High levels of SIRT1 expression as a protective mechanism against disease-related conditions. Front Endocrinol (Lausanne) 9: 614, 2018.
33. Hsu CP, Zhai P, Yamamoto T, Maejima Y, Matsushima S, Hariharan N, Shao D, Takagi H, Oka S and Sadoshima J: Silent information regulator 1 protects the heart from ischemia/reperfusion. Circulation 122: 2170-2182, 2010.
34. Xiong W, Ma Z, An D, Liu Z, Cai W, Bai Y, Zhan Q, Lai W, Zeng Q, Ren H and Xu D: Mitofusin 2 participates in mitophagy and mitochondrial fusion against angiotensin II-induced cardiomyocyte injury. Front Physiol 10: 411, 2019.
35. Mouchiroud L, Houtkooper RH, Moullan N, Katsyuba E, Ryu D, Cantó C, Mottis A, Jo YS, Viswanathan M, Schoonjans K, *et al*: The NAD(+)/sirtuin pathway modulates longevity through activation of mitochondrial UPR and FOXO signaling. Cell 154: 430-441, 2013.
36. Zhou Z, Ma D, Li P, Wang P, Liu P, Wei D, Wang J, Qin Z, Fang Q, Wang J, *et al*: Sirt1 gene confers Adriamycin resistance in DLBCL via activating the PCG-1α mitochondrial metabolic pathway. Aging (Albany NY) 12: 11364-11385, 2020.
37. Hu L, Guo Y, Song L, Wen H, Sun N, Wang Y, Qi B, Liang Q, Geng J, Liu X, *et al*: Nicotinamide riboside promotes Mfn2-mediated mitochondrial fusion in diabetic hearts through the SIRT1-PGC1α-PPARα pathway. Free Radical Biol Med 183: 75-88, 2022.
38. Soriano FX, Liesa M, Bach D, Chan DC, Palacín M and Zorzano A: Evidence for a mitochondrial regulatory pathway defined by peroxisome proliferator-activated receptor-gamma coactivator-1 alpha, estrogen-related receptor-alpha, and mitofusin 2. Diabetes 55: 1783-1791, 2006.
39. Sabouny R and Shutt TE: Reciprocal regulation of mitochondrial fission and fusion. Trends Biochem Sci 45: 564-577, 2020.
40. Liu YJ, McIntyre RL, Janssens GE and Houtkooper RH: Mitochondrial fission and fusion: A dynamic role in aging and potential target for age-related disease. Mech Ageing Dev 186: 111212, 2020.
41. Tao A, Xu X, Kvietys P, Kao R, Martin C and Rui T: Experimental diabetes mellitus exacerbates ischemia/reperfusion-induced myocardial injury by promoting mitochondrial fission: Role of down-regulation of myocardial Sirt1 and subsequent Akt/Drp1 interaction. Int J Biochem Cell Biol 105: 94-103, 2018.
42. Fu BC, Lang JL, Zhang DY, Sun L, Chen W, Liu W, Liu KY, Ma CY, Jiang SL, Li RK and Tian H: Suppression of miR-34a expression in the myocardium protects against ischemia-reperfusion injury through SIRT1 protective pathway. Stem Cells Dev 26: 1270-1282, 2017.
43. Liu P, Su J, Song X and Wang S: miR-92a regulates the expression levels of matrix metalloproteinase 9 and tissue inhibitor of metalloproteinase 3 via sirtuin 1 signaling in hydrogen peroxide-induced vascular smooth muscle cells. Mol Med Rep 17: 1041-1048, 2018.
44. Bae HJ, Noh JH, Kim JK, Eun JW, Jung KH, Kim MG, Chang YG, Shen Q, Kim SJ, Park WS, *et al*: MicroRNA-29c functions as a tumor suppressor by direct targeting oncogenic SIRT1 in hepatocellular carcinoma. Oncogene 33: 2557-2567, 2014.
45. Purohit PK, Edwards R, Tokatlidis K and Saini N: MiR-195 regulates mitochondrial function by targeting mitofusin-2 in breast cancer cells. RNA Biol 16: 918-929, 2019.
46. Zhang C, Nie P, Zhou C, Hu Y, Duan S, Gu M, Jiang D, Wang Y, Deng Z, Chen J, *et al*: Oxidative stress-induced mitophagy is suppressed by the miR-106b-93-25 cluster in a protective manner. Cell Death Dis 12: 209, 2021.
47. Qiu Y, Cheng R, Liang C, Yao Y, Zhang W, Zhang J, Zhang M, Li B, Xu C and Zhang R: MicroRNA-20b promotes cardiac hypertrophy by the inhibition of mitofusin 2-mediated inter-organelle Ca(2+) cross-talk. Mol Ther Nucleic Acids 19: 1343-1356, 2020.